Predicting the Effect of Dissolved Carbon Dioxide on the Glass Transition Temperature of Poly(Acrylic Acid)

Gui-Ping Cao[1,*], and George W. Roberts[2]

[1]*UNILAB, State-Key Laboratory of Chemical Engineering, East China University of Science and Technology, Shanghai 200237,China*

[2]*Department of Chemical and Biomolecular Engineering, North Carolina State University, Raleigh, NC 27695-7905*

Abstract The solubility of carbon dioxide (CO_2) in poly(acrylic acid) (PAA) at supercritical conditions was predicted using the Sanchez-Lacombe equation of state. The characteristic parameters of PAA were determined by fitting density data for the polymer above the glass transition temperature (T_g). The characteristic parameters of CO_2 were determined by fitting high-pressure pure component density data, and were compared with previously-determined values. The binary interaction parameter for the CO_2/PAA system was determined by fitting the measured sorption of CO_2 in PAA. The resulting model permits the solubility of CO_2 in PAA to be calculated at any set of conditions, which, in turn, allows Chow's Equation to be used to calculate the glass transition temperature. The predicted T_gs agree very well with measured values over a range of pressure from about 5 to 20 MPa of CO_2.

Keywords: Carbon dioxide, Poly(acrylic acid), Sanchez-Lacombe, glass transition, binary interaction parameter, Chow's equation

Introduction

Carbon dioxide, especially supercritical CO_2 ($scCO_2$), has been evaluated as an alternative to many organic chemicals that are used in synthesis and processing of polymers. The low cost, tunable properties, and environmentally-benign nature of $scCO_2$ have led to its use as a medium for polymer synthesis [1-4], for polymer precipitation by expansion from supercritical solutions [5-7], for polymerization reactions within CO_2-swollen polymers [8-11], for separations and fractionations [12], for impregnation of solutes into polymer matrices [13-15], for particle formation [16-18], for foaming [19-22], and for polymer blending [23-27]. Supercritical fluid technology has made tremendous strides in the past decade in terms of both commercial application [28, 29] and fundamental understanding of polymer/CO_2 interactions.

Many of the applications referenced above take advantage of the ability of CO_2 to penetrate into the space between polymer chains, and alter the chain mobility and free volume characteristics of the polymer matrix. Such variations in the microenvironment can be detected and evaluated by measurable physical properties, including CO_2 solubility, volumetric expansion, glass-transition temperature, viscosity, and interfacial tension. For example, high-pressure CO_2 can plasticize amorphous polymers, and consequently, depress their glass transition temperature, T_g, dramatically[30-37]. The reduction of T_g is due primarily to intermolecular interactions between CO_2 and the polymer.

A number of models have been established to describe fluid-polymer equilibrium. The review by Kirby and McHugh[38] provides a comprehensive discussion of the thermodynamic behavior of polymer-CO_2 systems. The Sanchez-Lacombe equation of state (SL-EOS) is probably the most widely used model to describe CO_2 solubility in various polymer systems [39-48]. In the SL-EOS, there are 4 characteristic parameters for each pure component: the characteristic temperature, T^*, the characteristic pressure, P^*, and the characteristic density, ρ^*, and the number of lattice sites, r, occupied by a molecule. As described in more detail below, these parameters may be determined from

*To Whom Correspondence Should Be Addressed: gpcao@ecust.edu.cn

pure-component experimental PVT data [44]. Characteristic parameters for CO_2 have been determined by a number of investigators, e.g., [43, 44, 46, 47].

Interest in understanding the behavior of precipitation polymerizations has been stimulated by use of supercritical CO_2 as a polymerization medium [4, 49, 50]. Liu and co-workers studied the precipitation polymerization of acrylic acid in scCO_2 to form poly(acrylic acid) (PAA) [4, 51-53]. Three different types of polymer morphology, and different particle sizes, were obtained, depending on whether the reaction temperature was below, close to, or above the glass transition temperature of the CO_2-PAA mixture. Particle size is a critical factor in many commercial applications of PAA, which include dispersants, thickeners, flocculants, and superabsorbent polymers. The authors [4] suggested that polymer morphology and particle size might be controlled through manipulation of the polymerization conditions, so as to adjust the relationship between T_g and the polymerization conditions. This idea, in turn, creates the need for a means to quantitatively describe the relationship between T_g, reaction temperature, and CO_2 pressure.

This paper deals with the solubility of CO_2 in PAA at supercritical conditions, and with the effect of the dissolved CO_2 on the T_g of the PAA/CO_2 mixture. The approach was as follows: (1) the characteristic parameters of CO_2 in the SL-EOS were determined over a wide range of temperature and pressure in the supercritical region by fitting PVT data for pure CO_2; (2) the characteristic parameters for PAA in the SL-EOS were determined by fitting PVT data for pure PAA, which has not been reported in the literature; (3) the binary interaction parameter for CO_2 and PAA was determined by fitting experimental data for the solubility of CO_2 in PAA; (4) the solubility of CO_2 in PAA was predicted at chosen conditions using the SL-EOS for the CO_2/PAA mixture, and; (5) the depression of T_g for CO_2-PAA mixtures was predicted from the calculated solubilities and compared to the experimental data[4].

Theory

As noted earlier, Sanchez and Lacombe have formulated a lattice fluid equation of state for pure fluids [47, 48] and their solutions[54]. The S-L EOS for a pure component is given by:

$$\tilde{\rho}^2 + \tilde{P} + \tilde{T}(\ln(1-\tilde{\rho}) + (1-1/r)\tilde{\rho}) = 0 \tag{1}$$

Here, $\tilde{T}$, $\tilde{P}$, and $\tilde{\rho}$ are the reduced temperature, pressure, and density, defined as $\tilde{T} \equiv T/T^*$, $\tilde{P} \equiv P/P^*$, and $\tilde{\rho} \equiv \rho/\rho^*$. The three parameters T^*, P^*, and ρ^* can be determined from experimental PVT data and the equation of the pure components. The parameter, r, is the number of lattice sites occupied by a molecule, which is related to the other three parameters and the molecular weight M of the pure component by $r = MP^*/RT^*\rho^*$ [55].

For polymers, $r \to \infty$, and $1/r \to 0$. For a mixture of a polymer and a penetrant, the characteristic parameters can be calculated from those for the pure components

$$1/r_m = \phi_1/r_1 + \phi_2/r_2 = \phi_1/r_1 \tag{2}$$

where ϕ_i is the volume fraction of component i in the mixture, the subscript i=1 corresponds to the penetratant, i=2 to the polymer, and i=m to the mixture. The n, the SL-EOS for the mixture is:

$$\tilde{\rho}_m^{\,2} + \tilde{P}_m + \tilde{T}_m(\ln(1-\tilde{\rho}_m) + (1-(\phi_1/r_1))\tilde{\rho}_m) = 0 \tag{3}$$

In eqn(3)., the value of P_m^* may be determined from the pure component parameters by

$$P_m^* = \phi_1 P_1^* + \phi_2 P_2^* - \phi_1\phi_2\Delta P_m^* \tag{4}$$

$$\Delta P_m^* = P_1^* + P_2^* - 2P_{12}^* \tag{5}$$

$$P_{12}^* = \psi\sqrt{P_1^* P_2^*} \tag{6}$$

In Eqn.(6), ψ is the binary interaction parameter, which is a measure of deviation of the mixture characteristic pressure from the geometric mean of the pure component characteristic pressures. The binary interaction parameter is commonly assumed to be unity when components are non-polar[43].

The value of the mixture characteristic temperature, T_m^*, is given by:

$$T_m^* = P_m^* / (\phi_1 P_1^* / T_1^* + \phi_2 P_2^* / T_2^*) \tag{7}$$

In order to determine the amount of penetrant sorbed into the polymer, the chemical potential of the penetrant in the pure phase is set equal to the chemical potential of the penetrant in the penetrant-polymer mixture.

$$\mu_{1,p} = \mu_{1,m} \tag{8}$$

This equality is based on the assumption that there is no polymer in the fluid phase. This assumption is generally valid except for certain fluoropolymers and silane polymers.

The chemical potential of penetrant in the pure phase is:

$$\mu_{1,p} = RTr_1\left(-\tilde{\rho}_1 / \tilde{T}_1 + \tilde{P}_1 / (\tilde{T}_1\tilde{\rho}_1) + (1-\tilde{\rho}_1)\ln(1-\tilde{\rho}_1)/\tilde{\rho}_1 + \ln\tilde{\rho}_1 / r_1\right) \tag{9}$$

and that in the penetrant-polymer mixture is,

$$\mu_{1,m} = RT(\ln\phi_1 + \phi_2 + (\tilde{\rho}_m(M_1/\rho_1^*)\chi\phi_2^2 + r_1[-\tilde{\rho}_m/\tilde{T}_1 + \tilde{P}_1/(\tilde{T}_1\tilde{\rho}_m) + (1-\tilde{\rho}_m)\ln(1-\tilde{\rho}_m)/\tilde{\rho}_m + \ln\tilde{\rho}_m / r]) \tag{10}$$

where, $\tilde{\rho}_m$ is given by eqn.(3). The parameter χ is defined as

$$\chi = \Delta P_m^* / RT \tag{11}$$

The weight fraction of penetrant, ω_1, and the close-packed volume fraction of penetrant, ϕ_1, in the mixture, have the following relationship

$$\omega_1 = \phi_1 / (\phi_1 + \phi_2(\rho_2^*/\rho_1^*)) \tag{12}$$

The solubility of a penetrant, e.g. CO_2, in a polymer can be measured through QCM[4].

If experimental solubility data is available, and if the characteristic parameters of the penetrant and polymer are specified, the binary interaction parameter ψ can be determined by minimizing the objective function:

$$s = \sum_{j=1}^{N_M} (\mu_{1,p,j} - \mu_{1,m,j})^2 \tag{13}$$

where N_M is the number of data points available. Then, the solubility of CO_2 in PAA over a wide range of temperature and pressure can be predicted through S-L EOS, and the depression of Tg of PAA can be predicted through Chow's equation[65].

Results and Discussion

Determination of Characteristic Parameters for CO_2

Kiszka et al [45] have suggested that the characteristic parameters for a fluid could be determined by fitting PVT data in the pressure and temperature range where predictions are desired. Table 1 is a brief summary of previously-determined characteristic parameters for CO_2, along with the ranges of temperature and pressure covered by the data from which these parameters were determined.

Table 1: Literature values of the characteristic parameters for CO_2

Ref.	T_1^*,K	P_1^*, atm	ρ_1^*,g/cm^3	r_1	T ,°C	P ,atm
[43]	316	4126	1.369	5.11	35	5-70
[44]	283	6510	1.62	7.6	25	1-70
[45]	305	5670	1.510	6.60	35-68	1-250
[46]	280	7101	1.6177	8.40	-56.6-31	0.51-73

The values of the parameters in Table 1 are quite different, possibly because of the different regions of temperature and pressure that were covered, and possibly because of different strategies for calculating the parameters from experimental data.

In this study of the CO_2/PAA equilibrium, the temperature range of interest is 45 to 95°C and the pressure range is 130 to 285 atm [4]. This region extends well beyond those covered by the studies in Table 1. Therefore, a re-evaluation of the characteristic parameters for CO_2 was necessary.

The characteristic parameters of CO_2 were obtained in this research by fitting the SL–EOS to

PVT data for CO_2 in the range of T from 45 to 95°C, and in the range of P from 130 to 285 atm. The objective function minimized was:

$$s_\rho = \sum_{j=1}^{N_M} (\rho_{1,\exp,j} - \rho_{1,\mathrm{mod},j})^2 \tag{14}$$

Here, N_M is the total number of data points, $\rho_{1,\exp,j}$ is the experimental value of the CO_2 density at temperature T_j and pressure P_j,; $\rho_{1,\mathrm{mod},j}$ is the value of the CO_2 density at temperature T_j and pressure P_j, as calculated from the SL-EOS for pure CO_2, Eqn.(1), given values of the parameters T_1^* P_1^*, ρ_1^*, and r_1.

Final values of the characteristic parameters, T_1^* P_1^*, ρ_1^*, and r_1, determined by this method are shown in Table 2. The experimental data was obtained from NIST [56].

Table 2: Characteristic parameters of CO_2 obtained by non-linear regression of NIST [51] data (P=130 to 280 atm; T=45 to 95°C)

T_1^*, K	P_1^*, atm	ρ_1^*, g/cm^3	r_1
327	4476	1.46	5.19

Figure 1 shows a comparison of the calculated and experimental PVT data for CO_2. Visually, the experimental data agree well with the calculated values. The standard variation of density is:

$$\sigma_\rho = \sqrt{s_\rho/(N_M - 1)} = 5.25 \times 10^{-3} \ \mathrm{g/cm^3}$$

This value, a measure of the agreement between the NIST data and the density predicted by the SL-EOS, is quite small compared to the actual densities of CO_2 in the experimental region of this study.

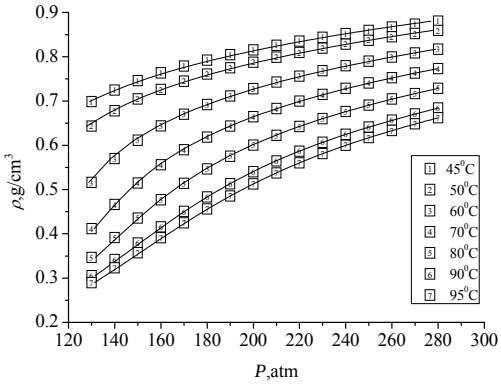

Figure 1 Density of CO_2 versus CO_2 pressure at different temperatures. Symbols: density values from NIST [56]. Lines: densities calculated from the SL-EOS using the characteristic parameters in Table 2.

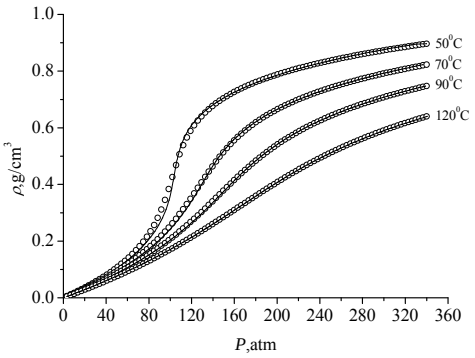

Figure 2 Density of CO_2 versus pressure over a wider range of temperature and pressure. Symbols: density values from NIST [56]. Lines: densities calculated from the SL-EOS using the characteristic parameters in Table 2.

In order to check whether the characteristic parameters in Table 2 can be used over a wider range of temperature and pressure, the density of CO_2 was calculated using these parameters, over a range of temperature from 50 to 120°C, and a pressure range from 3.4 atm to 340 atm. Figure 2 is a comparison of the NIST data with calculations using the SL-EOS with the characteristic parameters given in Table 2. The calculated densities over the wider range of conditions agree well with the NIST data.

Evaluation of Characteristic Parameters for PAA

Characteristic parameters for PAA have not been reported previously. The parameters used in this paper were determined by fitting the SL-EOS to experimental data for PAA above the glass transition temperature. Zoller and Walsh[58] have reported experimental PVT data for PAA in the temperature range from 23.4 to 224.3°C and in the pressure range from 0 to 200 MPa for intervals of 20MPa. The most relevant pressure range for the present study is 6.5 to 28MPa, making it difficult to use the data

directly. Therefore, the Tait equation[59, 60] was fit to the data, and was used to interpolate with respect to temperature and pressure.

Different forms of the Tait equation have been used to represent the PVT behavior for a number of liquids, including polymeric liquids [59, 61-63]. The equation used here is:

$$\rho_0 / \rho = 1 - c \ln\{1 + P/(b_1 \exp(-b_2 T))\} \quad (15)$$

In eqn.(15), ρ is the density at pressure P and temperature T; ρ_0 is the density at P=1 bar and the same temperature (T); and c, b_1 and b_2 are constants. These constants were determined for PAA in the region above T_g by non-linear regression of the data of Zoller and Walsh. The resulting values are shown in Table 3.

Figure 3 shows the fit of the Tait equation to the experimental data for PAA above T_g. The PAA densities calculated from the Tait equation fit the experimental data quite well.

The "data" that is required to determine the characteristic parameters for PAA in the pressure range from 6.5 to 30.0MPa was calculated from Eqn.(15). Then, the characteristic parameters in the SL-EOS were obtained by non-linear regression. Table 4 gives the final values of the characteristic parameters for pure PAA above T_g.

Table 3: Parameters for PAA in the Tait equation ($T > T_g$)

T, °C	P, MPa	c ($\times 10^2$)	B_1 ($\times 10^{-3}$), bars	b_2 ($\times 10^3$),K^{-1}
24.3-224.3	0-200	7.1138	7.1132	2.7284

Table 4 Characteristic parameters in the SL-EOS for pure PAA above T_g

T_2^*,K	P_2^*,atm	ρ_2^*,g/cm^3
859	9250	1.483

Figure 4 shows a comparison of the PAA densities calculated from the SL-EOS using these parameters with the "experimental" data from the Tait equation. The densities calculated from the SL-EOS match the "experimental" data quite well. In subsequent calculations, the average values of T_2^*, P_2^*, and ρ_2^* shown in Table 4 have been used.

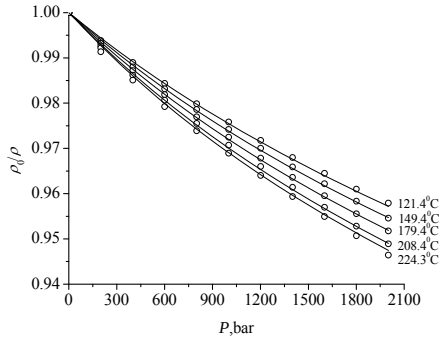

Figure 3 Fit of the Tait equation to density data for PAA above T_g.

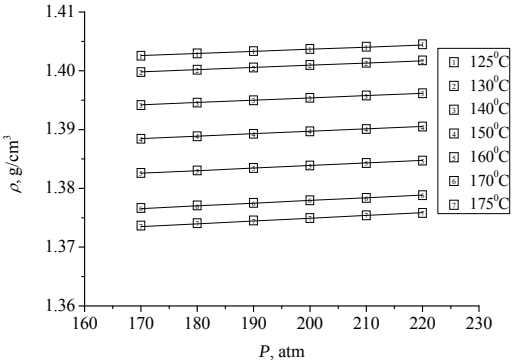

Figure 4 Comparison of calculated PAA density with the "experimental" PAA density. Symbol: "experimental" density from the Tait equation. Line: calculated density from SL-EOS using the characteristic parameters in Table 6.

The binary interaction parameter for the CO_2/PAA mixture

The value of ψ for CO_2-PAA mixtures was obtained by fitting experimental data for the solubility of CO_2 in PAA. The experimental solubility data of CO_2 in PAA were obtained from T. Liu et al.[4]. Twenty data points were available.

The optimal value of the binary interaction parameter, ψ, was determined to be 1.0299, slightly larger than 1. Condo et al. [64] have shown that the binary interaction parameter has a major influence on the solubility of the penetrant in the polymer, and sequentially, on the variation of T_g with penetrant pressure. Figure 5 shows the experimental and calculated solubilities of CO_2 in PAA over the temperature range from 50 to 90 °C and the pressure range from 68 to 272 atm. The calculated and experimental solubilities agree reasonably well.

Figure 6 shows the relationship of the objective function, s, and the binary mixing parameter, ψ.

A small change of the value of ψ leads to a large change of s in equ(13). In order to investigate how the predicted solubility of CO_2 in PAA changes with the value of ψ, the solubility of CO_2 in PAA was calculated at different assumed values of ψ, except for 1.0299. Figure 7 shows the results. The solubility of CO_2 in PAA is very sensitive to the values of binary interaction parameter, and increases significantly as ψ is increased, as noted by Condo et al. [64]. Clearly, an accurate value of ψ is necessary to predict the solubility correctly.

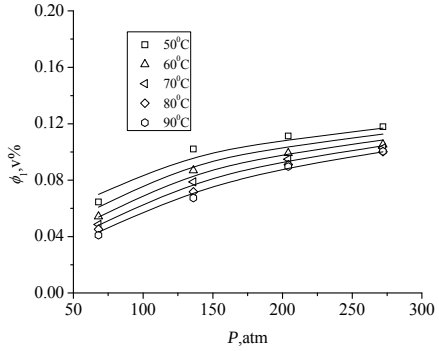

Figure 5 Experimental and calculated solubility of CO_2 in PAA. (ψ=1.0299. Points are experimental data[4]; lines are calculations using the SL-EOS)

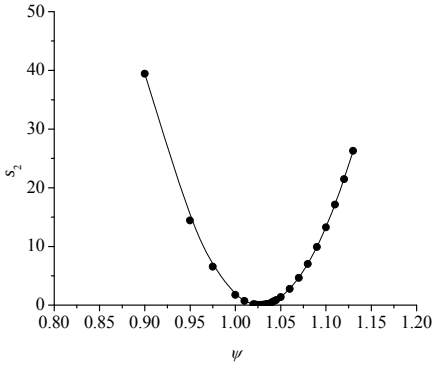

Figure 6 The objective function s versus the binary interaction parameter, ψ

Predictions of the solubility of CO_2 in PAA

The solubility of CO_2 in "rubbery" PAA can be calculated using the characteristic parameters of CO_2: T_1^*, P_1^*, ρ_1^*, and r_1, the characteristic parameters of PAA: T_2^*, P_2^*, and ρ_2^*, and the binary interaction parameter of CO_2 and PAA, ψ. The solubility of CO_2 in PAA was calculated by using the model over an extended temperature and pressure range, from 60 to 150 °C and 3.4 to 340 atm. The reported T_g of pure PAA is about 120.9°C[4]. Strictly speaking, the characteristic parameters for PAA in Table 4 are not valid below this temperature, since these parameters were determined from data in the rubbery region. Nevertheless, the solubility calculations have been extended to temperatures below 120.9°C to allow for the reduction of T_g by dissolved CO_2.

Figure 8 shows the predicted isothermal solubility of CO_2 in PAA versus pressure. Below the critical pressure of CO_2, i.e., when the fluid phase is a gas, the predicted volume fraction of CO_2 in the polymer (ϕ_1) increases rapidly with pressure and is relatively linear in pressure. Above the critical pressure, ϕ_1 still increases with pressure, but the slope of the curve is lower. There is no suggestion of an asymptote in ϕ_1 with increasing pressure at any of the temperatures investigated.

As temperature increases, the volume fraction of CO_2 decreases at any given pressure, as expected. Chow[65] has proposed a means to calculate the depression of T_g due to a dissolved component as follows

$$\ln(T_{g,mix} / T_{g,0}) = \beta[\theta \ln \theta + (1-\theta)\ln(1-\theta)] \tag{16}$$

where,

$$\theta = M_u /(zM_d)\omega_1 /(1-\omega_1) \tag{17}$$

$$\beta = zR /(M_u \Delta C_{pp}) \tag{18}$$

In Eqns.(16), (17) and (18), $T_{g,mix}$ is the glass-transition temperature of the polymer containing a weight fraction, ω_1, of the penetrant; $T_{g,0}$ is the glass-transition temperature of the pure polymer; M_u is the molar mass of the polymer repeat unit; M_d is the molar mass of the penetrant; R is the gas constant; ΔC_{pp} is the excess transition isobaric specific heat of the pure polymer, and; z is the lattice coordination number, which can be either 1 or 2. For polymers with small repeat units, such as polystyrene and poly(methyl methacrylate), z = 1 gives the best fit of the experimental results. For polymers with larger repeat units, such as polycarbonate and poly(ethylene terephthalate), z = 2 usually gives a better

description of the data[34, 36, 66-68]. Liu et al.[4] reported that Chow's equation agreed well with the experimental data when: $z = 1$; $T_{g,0}$=120.9°C; and; ΔC_{pp}=0.4J/(g °C).

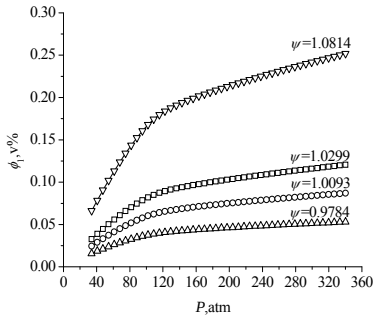

Figure 7 The effect of errors in ψ on the solubility of CO_2 in PAA (T = 60 °C).

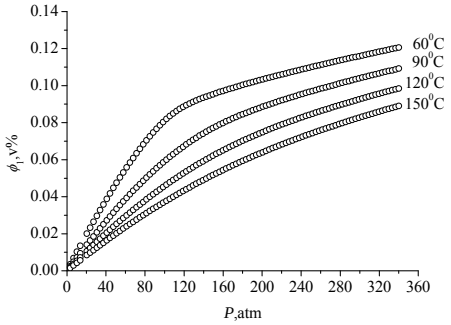

Figure 8 Predicted solubility of CO_2 in PAA at various temperatures and pressures

The glass-transition temperature of the CO_2-PAA mixture was calculated using eqn.(16). The results are shown in Figure 9. The calculations were performed by choosing a temperature and CO_2 pressure, calculating ϕ_1 at these conditions, as described in the previous section, and then calculating ω_1 from Eqn.(12). Two of the temperatures shown in Figure 9 (60 and 90°C) are well below the glass-transition temperature of the pure polymer. The polymer is glassy at these conditions if no CO_2 is dissolved in it. Therefore, the calculations of ω_1 and T_g at these conditions are approximate, since the characteristic parameters for PAA were derived from data in the rubbery region. However, as the CO_2 pressure is increased, the predicted value of T_g decreases. At 90 °C and a CO_2 pressure of about 80 atm, the value of T_g has decreased to 90 °C. Above this CO_2 pressure, the polymer is rubbery if the temperature is 90°C.

At 60°C and a CO_2 pressure of 340 atm, the predicted glass-transition temperature of the polymer has dropped to about 65 °C. However, the polymer remained "glassy" over this whole range of pressure. Therefore, the predicted glass-transition temperatures are approximate at this temperature, over the range of pressure considered.

Another presentation of the effect of CO_2 pressure on the glass-transition temperature is shown in Figure 10. The lines labeled with temperatures are the isopleths of $T_{g,mix}$. On one of these lines, the solubility, ϕ_1, and therefore the glass transition temperature, $T_{g,mix}$, are constant, i.e., at any point on an isopleth, the temperature and pressure are such that the CO_2 solubility remains unchanged.

The circular symbols on the isopleths mark the points where the temperature and T_g are equal. These points define the boundary between the rubbery and glassy regions, as shown in Figure 10. Experimental values of $T_{g,mix}$[4] also are shown in the figure. The experimental data agree well with the predicted values.

Condo et al.[64] and Kikic et al. [69] defined four types of glass-transition behavior for CO_2-polymer mixtures, depending on the value of the binary interaction parameter, ψ. With increasing ψ, the glass-transition behavior type changes from Type I through Types II and III to Type IV. With Type I behavior, there is a minimum in the T_g versus pressure curve. Under certain conditions, two glass transitions can be observed as the pressure is reduced at constant temperature. This behavior is relevant to the PAA/CO_2 system, since T_g was measured by decreasing the pressure isothermally [4]. Note also that Chow's equation predicts that T_g will go through a minimum at $\theta = 0.50$, which corresponds to ω_1 = 0.23 for PAA.

Calculations with the solubility model developed in the previous section show that the T_g minimum occurs at CO_2 pressures in excess of 1500atm. for PAA, which is showed in figure 11. The initial pressure for the experiments of Reference 4 was about 100 atm. This is in the rubbery region for all of the temperatures that were studied experimentally. Therefore, only one T_g would be observed in the type of experiment that was conducted.

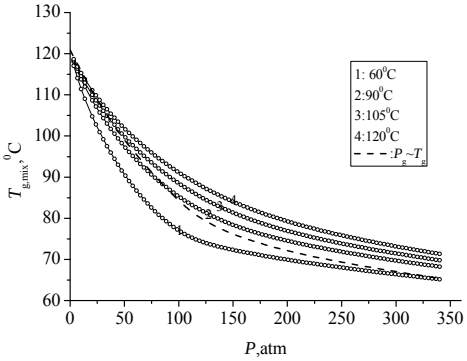

Figure 9 Depression of the glass-transition temperature of PAA by dissolved CO_2. The abscissa is the pressure of CO_2.

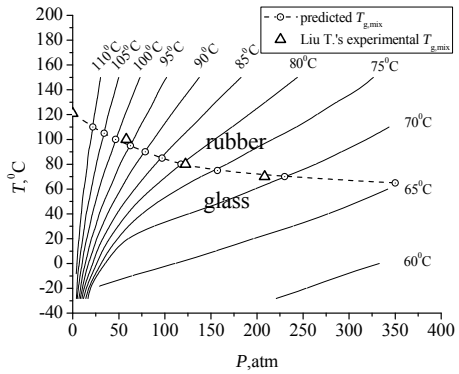

Figure 10 Theoretical glass transition temperature isopleths. The solid lines are the $T_{g,mix}$ isopleths of the CO_2-PAA mixture. The dashed line with hollow round points is the locus of predicted $T_{g,mix}$ values with a PAA normal $T_{g,0}$ =120.9°C. The triangular points are the experimental $T_{g,mix}$ values from [4]. The binary interaction parameter is 1.0299.

Conclusions

The Sanchez-Lacombe equation of state (SL-EOS) was demonstrated to be a robust thermodynamic model for describing the CO_2-PAA system at supercritical conditions. The characteristicparameters of CO_2 in the SL-EOS were determined over a wide range of temperature and pressure in the supercritical region by fitting density data from NIST. The characteristic parameters for PAA, above the glass-transition temperature and over a wide range of pressure, were determined by fitting previously-measured densities. The binary interaction parameter in the SL-EOS was determined by fitting data for the sorption of CO_2 in PAA. The CO_2 solubility in PAA is very sensitive to the value of the binary interaction parameter.

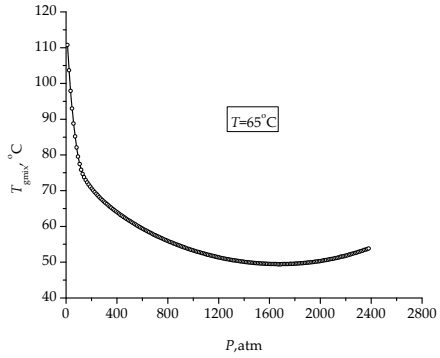

Figure 11 Type I *T*g of PAA versus pressure behavior

The resulting model permitted the major thermodynamic properties of CO_2-PAA mixtures, namely the CO_2 solubility and the scCO_2-induced polymer swelling to be predicted. Chow's Equation then could be used to predict the dependence of the glass-transition temperature of PAA on theCO_2 pressure. These predictions agreed with measured values of T_g. The T_g of CO_2-PAA mixtures is predicted to decrease from 121 °C to 65 °C as the CO_2 pressure is increased from 0 to 35 MPa. The glass-transition temperature is predicted to exhibit Type I behavior.

The characteristic parameters for CO_2, determined here by fitting high-pressure density data, were compared with four other published sets of characteristic parameters, determined from lower-pressure data. The previously-determined parameters did not lead to accurate predictions of CO_2 behavior at the higher temperatures and pressures considered here. However, the new characteristic parameters were able to describe the properties of CO_2 at lower temperatures and pressures about as well as the existing parameters.

Acknowledgements

The first author (GPC) was a senior visiting scholar supported by the China Scholarship Council (CSC-2005831073). Partial support for the research also was provided by the National Nature Science Foundation of China (NSFC-20676031) and by the STC Program of the National Science Foundation under Agreement No. CHE-9876674.

The authors thank Professor Ruben G. Carbonell and Dr. Tao Liu for their help.

References

1. J.M. Desimone, E.E. Maury, Y.Z. Menceloglu, J.B. McClain, T.J. Romack, and J.R. Combes, Dispersion Polymerizations in Supercritical Carbon Dioxide. Science, 1994. **265**(5170): 356-359.
2. M.R. Clark and J.M. DeSimone, Cationic Polymerization of Vinyl and Cyclic Ethers in Supercritical

and Liquid Carbon Dioxide. Macromolecules, 1995. **28**(8): 3002-3004.
3. F.A. Adamsky and E.J. Beckman, Inverse emulsion polymerization of acrylamide in supercritical carbon dioxide. Macromolecules, 1994. **27**(1): 312-314.
4. T. Liu, P. Garner, J.M. DeSimone, G.W. Roberts, and G.D. Bothun, Particle formation in precipitation polymerization: Continuous precipitation polymerization of acrylic acid in supercritical carbon dioxide. Macromolecules, 2006. **39**(19): 6489-6494.
5. J.W. Tom and P.G. Debenedetti, Formation of bioerodible polymeric microspheres and microparticles by rapid expansion of supercritical solutions. Biotechnology Progress, 1991. **7**(5): 403-411.
6. S. Mawson, K.P. Johnston, J.R. Combes, and J.M. DeSimone, Formation of Poly (1, 1, 2, 2-tetrahydroperfluorodecyl acrylate) Submicron Fibers and Particles from Supercritical Carbon Dioxide Solutions. Macromolecules, 1995. **28**(9): 3182-3191.
7. G. Luna-Barcenas, S.K. Kanakia, I.C. Sanchez, and K.P. Johnston, Semicrystalline microfibrils and hollow fibres by precipitation with a compressed-fluid antisolvent. Polymer, 1995. **36**(16): 3173-3182.
8. J.J. Watkins and T.J. McCarthy, Polymerization in Supercritical Fluid-Swollen Polymers: A New Route to Polymer Blends. Macromolecules, 1994. **27**(17): 4845-4847.
9. J.J. Watkins and T.J. McCarthy, Polymerization of Styrene in Supercritical CO_2-Swollen Poly (chlorotrifluoroethylene). Macromolecules, 1995. **28**(12): 4067-4074.
10. G.H. Li, Q.M. Pan, G.L. Rempel, and F.T.T. Ng, Effect of supercritical CO2 on bulk hydrogenation of nitrile butadiene rubber catalyzed by RhCl(PPh3)(3). Macromolecular Symposia, 2003. **204**: 141-149.
11. G.L. Rempel, G.H. Li, Q.M. Pan, and F.T.T. Ng, A "green" technique for high performance elastomers - Fundamental investigation for hydrogenation of nitrile butadiene rubber in supercritical carbon dioxide. Macromolecular Symposia, 2002. **186**: 23-28.
12. M.A. McHugh and V.J. Krukonis, Supercritical Fluid Extraction: Principles and Practice. 1994: Butterworth-Heinemann.
13. A.I. Cooper, Polymer synthesis and processing using supercritical carbon dioxide. Journal of Materials Chemistry(UK), 2000. **10**(2): 207-234.
14. S.G. Kazarian, N.H. Brantley, and C.A. Eckert, Dyeing to be clean: Use supercritical carbon dioxide. Chemtech, 1999. **29**(7): 36-41.
15. S.G. Kazarian, Polymer processing with supercritical fluids. Polymer Science, Series C: Chemistry Reviews(USA), 2000. **42**(1): 78-101.
16. R. Thiering, F. Dehghani, and N.R. Foster, Current issues relating to anti-solvent micronisation techniques and their extension to industrial scales. Journal of Supercritical Fluids, 2001. **21**(2): 159-177.
17. B. Bungert, G. Sadowski, and W. Arlt, Separations and material processing in solutions with dense gases. Ind. Eng. Chem. Res, 1998. **37**(8): 3208?220.
18. E. Reverchon, Supercritical antisolvent precipitation of micro- and nano-particles. Journal of Supercritical Fluids, 1999. **15**(1): 1-21.
19. K.C. Frisch and D. Klempner, Handbook of Polymeric Foams and Foam Technology. 1991: Distributed in USA and Canada by Oxford University Press.
20. A.H. Landrock, Handbook of Plastic Foams. 1995: Noyes Data Corporation/Noyes Publications.
21. K.C. Khemani, Polymeric foams: science and technology(Orlando FL, 25-29 August 1996). A. C. S. symposium series.
22. S.T. Lee and S.T. Lee, Foam Extrusion. 2000: CRC Press.
23. R.D. Deanin and M.A. Manion, Compatibilization of Polymer Blends. Polymer Blends and Alloys, Shonaike, GO and Simon, PO (eds.), Marcel Dekker Inc., New York, 1999.
24. U. Sundararaj and C.W. Macosko, Drop Breakup and Coalescence in Polymer Blends - the Effects of Concentration and Compatibilization. Macromolecules, 1995. **28**(8): 2647-2657.
25. J.K. Lee and C.D. Han, Evolution of polymer blend morphology during compounding in an internal mixer. Polymer, 1999. **40**(23): 6277-6296.
26. J.K. Lee and C.D. Han, Evolution of polymer blend morphology during compounding in a twin-screw extruder. Polymer, 2000. **41**(5): 1799-1815.
27. M. Lee, C. Tzoganakis, and C.B. Park, Extrusion of PE/PS blends with supercritical carbon dioxide. Polymer Engineering & Science, 1998. **38**(7): 1112-1120.

28. J. Watkins, Supercritical fluid technology for the fabrication of functional nanostructure films and devices. 8th International Symposium on Supercritical Fluids,ISSF2006(Plenary Lecture), 2006: 3.
29. M. Poliakoff, A new phase in supercritical chemistry. 8th International Symposium on Supercritical Fluids,ISSF2006(Plenary Lecture), 2006: 4~5.
30. Q. Zhang, M. Xanthos, and S.K. Dey, In-line measurement of gas solubility in polystyrene and polyethylene terephthalate melts during foam extrusion. ASME Cell Microcellular Mater, 1998: 75?3.
31. M.L. O'Neill and Y.P. Handa, In Assignment of the Glass Transition. ASTM STP, 1994. **1249**.
32. Y. Kamiya, K. Mizoguchi, and Y. Naito, A Dielectric-Relaxation Study of Plasticization of Poly(Ethyl Methacrylate) by Carbon-Dioxide. Journal of Polymer Science Part B-Polymer Physics, 1990. **28**(11): 1955-1964.
33. Y. Mi and S. Zheng, A new study of glass transition of polymers by high pressure DSC. Polymer(Guildford), 1998. **39**(16): 3709-3712.
34. Y.P. Handa, S. Lampron, and M.L. Oneill, On the Plasticization of Poly(2,6-Dimethyl Phenylene Oxide) by CO2. Journal of Polymer Science Part B-Polymer Physics, 1994. **32**(15): 2549-2553.
35. Z. Zhang and Y.P. Handa, An in situ study of plasticization of polymers by high-pressure gases. J Polym Sci: Part B: Polym Phys, 1998. **36**: 977-982.
36. J.S. Chiou, J.W. Barlow, and D.R. Paul, Plasticization of Glassy Polymers by CO_2. Journal of Applied Polymer Science, 1985. **30**: 2633-2642.
37. R.R. Edwards, Y. Tao, S. Xu, P.S. Wells, K.S. Yun, and J.F. Parcher, Chromatographic investigation of the effect of dissolved carbon dioxide on the glass transition temperature of a polymer and the solubility of a third component(additive). Journal of Polymer Science Part B Polymer Physics, 1998. **36**(14): 2537-2549.
38. C.F. Kirby and M.A. McHugh, Phase Behavior of Polymers in Supercritical Fluid Solvents. Chem Rev, 1999. **99**(2): 565-602.
39. D.H. Liu, H.B. Li, M.S. Noon, and D.L. Tomasko, CO_2-induced PMMA swelling and multiple thermodynamic property analysis using Sanchez-Lacombe EOS. Macromolecules, 2005. **38**(10): 4416-4424.
40. M. Pantoula and C. Panayiotou, Sorption and swelling in glassy polymer/carbon dioxide systems. Part I. Sorption. The Journal of supercritical fluids, 2006. **37**(2): 254-262.
41. E.C. Voutsas, G.D. Pappa, K. Magoulas, and D.P. Tassios, Vapor liquid equilibrium modeling of alkane systems with Equations of State:"Simplicity versus complexity". Fluid Phase Equilibria, 2006. **240**(2): 127-139.
42. H. Park, C.B. Park, C. Tzoganakis, K.H. Tan, and P. Chen, Surface Tension Measurement of Polystyrene Melts in Supercritical Carbon Dioxide. Ind. Eng. Chem. Res, 2006. **45**(5): 1650-1658.
43. R. Hariharan, B.D. Freeman, R.G. Garbonell, and G.C. Sarti, Equation of state predictions of sorption isotherms in polymeric materials. Journal of applied polymer science, 1993. **50**(10): 1781-1795.
44. D.S. Pope, I.C. Sanchez, W.J. Koros, and G.K. Fleming, Statistical thermodynamic interpretation of sorption/dilation behavior of gases in silicone rubber. Macromolecules, 1991. **24**(8): 1779-1783.
45. M.B. Kiszka, M.A. Meilchen, and M.A. McHugh, Modeling high-pressure gas polymer mixtures using the sanchez-lacombe equation of state. Journal of Applied Polymer Science, 1988. **36**(3): 583-597.
46. P.K. Kilpatrick and S.H. Chang, Saturated Phase-Equilibria and Parameter-Estimation of Pure Fluids with 2 Lattice-Gas Models. Fluid Phase Equilibria, 1986. **30**: 49-56.
47. I.C. Sanchez and R.H. Lacombe, An elementary molecular theory of classical fluids. Pure fluids. The Journal of Physical Chemistry, 1976. **80**(21): 2352-2362.
48. I.C. Sanchez and R.H. Lacombe, An elementary equation of state for polymer liquids. Journal of Polymer Science Polymer Letters Edition, 1977. **15**(2): 71-75.
49. D.A. Canelas and J.M. DeSimone, Polymerizations in liquid and supercritical carbon dioxide. Adv Polym Sci, 1997. **133**: 103.
50. M. McCoy, Biocatalysis grows for drug synthesis. Chem. Eng. News, 1999. **77**(1): 10-13.
51. T. Liu, J.M. Desimone, and G.W. Roberts, Continuous Precipitation Polymerization of Acrylic Acid in Supercritical Carbon Dioxide: The Polymerization Rate and the Polymer Molecular Weight. Journal of Polymer Science, Part A, Polymer Chemistry, 2005. **43**(12): 2546-2555.

52. T. Liu, J.M. DeSimone, and G.W. Roberts, Kinetics of the precipitation polymerization of acrylic acid in supercritical carbon dioxide: The locus of polymerization. Chemical Engineering Science, 2006. **61**(10): 3129-3139.
53. T. Liu, J.M. DeSimone, and G.W. Roberts, Cross-linking polymerization of acrylic acid in supercritical carbon dioxide. Polymer, 2006. **47**(12): 4276-4281.
54. R.H. Lacombe and I.C. Sanchez, Statistical Thermodynamics of Fluid Mixtures. Journal of Physical Chemistry, 1976. **80**(23): 2569-2580.
55. I.C. Sanchez and R.H. Lacombe, Statistical Thermodynamics of Polymer-Solutions. Macromolecules, 1978. **11**(6): 1145-1156.
56. NIST, Thermophysical Properties of Fluid Systems. http://webbook.nist.gov/chemistry/fluid/. 2005.
57. K.J. Beers, Numerical Methods for Chemical Enineering, Cambridge Press. 2006.
58. P. Zoller, D.J. Walsh, and W. Walsh, Standard Pressure-Volume-Temperature Data for Polymers. 1995: CRC Press.
59. A. Quach and R. Simha, Pressure-Volume-Temperature Properties and Transitions of Amorphous Polymers; Polystyrene and Poly (orthomethylstyrene). Journal of Applied Physics, 1971. **42**(12): 4592-4606.
60. S. Beret and J.M. Prausnitz, Densities of Liquid Polymers at High Pressure. Pressure-Volume-Temperature Measurements for Polythylene, Polyisobutylene, Poly (vinyl acetate), and Poly (dimethylsiloxane) to 1 kbar. Macromolecules, 1975. **8**(4): 536-538.
61. M.S. Benson and J. Winnick, PVT properties of liquid n-octane. Journal of Chemical and Engineering Data, 1971. **16**(2): 154-157.
62. H.E. Eduljee, D.M. Newitt, and K.E. Weale, Pressure Volume Temperature Relations in Liquids and Liquid Mixtures .1. the Compression of Normal-Hexane, Normal-Heptane, Normal-Octane, and of Their Binary and Ternary Mixtures, up to 5000 Atmospheres. Journal of the Chemical Society, 1951(NOV): 3086-3091.
63. D.P. Maloney and J.M. Prausnitz, Thermodynamic properties of liquid polyethylene. Journal of Applied Polymer Science, 1974. **18**(9): 2703-2710.
64. P.D. Condo, I.C. Sanchez, C.G. Panayiotou, and K.P. Johnston, Glass transition behavior including retrograde vitrification of polymers with compressed fluid diluents. 1992, American Chemical Society. 6119-6127.
65. T.S. Chow, Molecular Interpretation of the Glass Transition Temperature of Polymer-Diluent Systems. 1980, American Chemical Society. 362-364.
66. Y.P. Handa, S. Capowski, and M. Oneill, Compressed-Gas-Induced Plasticization of Polymers. Thermochimica Acta, 1993. **226**: 177-185.
67. T. Banerjee and G.C. Lipscomb, Direct measurement of the carbon dioxide-induced glass transition depression in a family of substituted polycarbonates. Journal of Applied Polymer Science, 1998. **68**(9): 1441-1449.
68. J.S. Chiou and D.R. Paul, Sorption and Transport of CO_2 in PVF_2/PMMA Blends. Journal of Applied Polymer Science, 1986. **32**(1): 2897-2918.
69. I. Kikic, F. Vecchione, P. Alessi, A. Cortesi, F. Eva, and N. Elvassore, Polymer plasticization using supercritical carbon dioxide: Experiment and modeling. Industrial & Engineering Chemistry Research, 2003. **42**(13): 3022-3029.